JOURNAL OF MATERIALS SCIENCE **34** (1999) 3623–3630

Effect of environmental factors on thermal shock behaviour of polycrystalline alumina ceramics

BONG SEOK HAHN, HONG LIM LEE
Department of Ceramic Engineering, Yonsei University, Seoul, 120-749, Korea
E-mail: html1@bubble.yonsei.ac.kr

The effect of the environmental factors on thermal shock behaviour of polycrystalline alumina ceramics was studied by quenching the alumina specimens into various quenching media. The environment factors of quenching media were controlled by changing the temperature of water and changing the concentration of the propylene glycol/water solution. The convection heat transfer coefficient and thermal stress increased as the temperature of cooling water increased and decreased as the concentration of the propylene glycol in water increased. The critical thermal stress which makes the cracks grow catastrophically was found to be generated by the critical cooling rate, and the critical cooling rate of alumina ceramics was found to be a certain value (550 °C/s) and same for all cooling liquids. Therefore, cooling rate was found to be the most influential of the environmental factors in thermal shock.

1. Introduction

The investigation of the thermal shock for ceramics so far has been carried out mainly to find the strength degradation and crack growth mechanism [1, 2]. Thermal shock behavior is affected by many environment factors on thermal shock. Therefore, the study about the effect of environmental factors on thermal shock behaviour is needed.

Thermal shock is caused by the thermal stress, which is generated by the temperature gradient between the surface and the inside of a solid specimen immersed in the quenching media [3]. However, the most important environmental factor which affects significantly on temperature gradient in the solid specimen during thermal shock is considered to be the cooling rate of the specimen. The cooling rate of the specimen is also affected by many factors of the cooling process including the temperature of the cooling liquid, the concentration of the components in the cooling liquid solution, the relative velocity of the motion of the specimen in the fluid, the roughness of the surface of the specimen, etc. [4]. These factors of the cooling process are considered to determine the heat transfer rate between the solid surface and the cooling liquid.

Heat transfer between the solid surface and the fluid mainly takes place by convection mechanism and, hence, the heat transfer coefficient is very important in thermal shock tests [5]. Heat transfer coefficient depends on the environmental factors of the quenching media, the geometry of the solid specimen, the physical properties of the fluid, temperature and pressure, etc. The studies about the effect of the environmental factors on thermal shock are not so many and the data so far obtained are not sufficient for explaining the thermal shock phenomena of ceramics [6–9].

In this study, the effects of environmental factors on thermal shock test of ceramics were investigated by direct measurement of cooling temperature variation of Al_2O_3 specimens during thermal quenching using various cooling liquids. Temperature variation of the specimen surface indicates the variation of the environmental factors which the specimen suffers during thermal shock test. The temperature variation of the specimen surface is related to the heat transfer coefficient, which again is related to the cooling rate of the specimen. The cooling rate is considered definitely to determine the critical thermal stress, which leads to the failure of the solid specimens.

2. Experimental

2.1. Quenching media

To study the effect of the environmental factors on thermal shock, the temperature of distilled water and the concentration of propylene glycol/water solution were varied. The temperature of distilled water was varied by the water bath. Fig. 1 is the well-known boiling curve [10], showing a schematic view of the convection heat transfer coefficient variation according to the temperature difference of the heated solid specimen and the cooling water when the specimen was immersed in water. Regions I, II, III classify the regimes of boiling phenomena of water. The variation of the convection heat transfer coefficient of water according to the temperature of water, as shown in Fig. 1, will be considered to explain the thermal shock behaviour of the alumina ceramics in this study. Hence, the temperature of the cooling water was controlled over the temperature range; 4, 20, 40, 60, 80 and 100 °C during quenching.

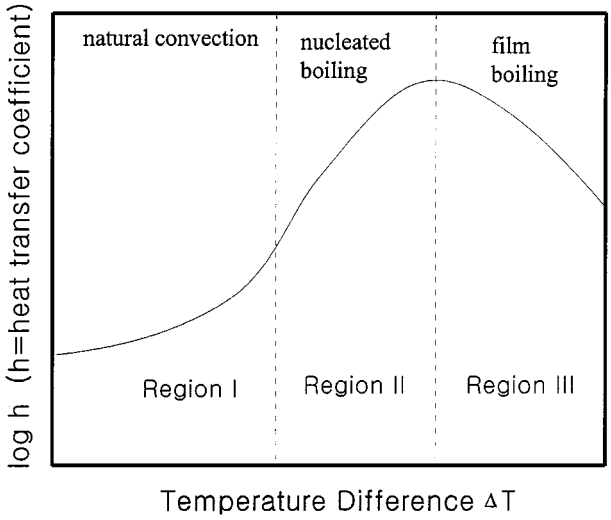

Figure 1 Schematic representation of the heat transfer coefficient variation of water as a function of temperature difference.

Propylene glycol is completely miscible with water over whole range of compositions and their mixture is used as the antifreezing solution. The thermal conductivity of propylene glycol (200 W/m · °C at 25 °C) is much lower than that of water (600 W/m · °C at 25 °C) [11]. The convection heat transfer coefficient of propylene glycol is considered to be much lower than that of pure water, so that the convection heat transfer coefficient of propylene glycol/water solution is considered to be lower than that of pure water but higher than that of propylene glycol. The concentration of propylene glycol in water used for thermal shock test was varied over the range; 0, 25, 50 and 75 vol %.

2.2. Thermal shock test

Thermal shock test was carried out in various quenching media; distilled water and various concentrations of propylene glycol in water. Polycrystalline alumina rectangular bar specimens of $4 \times 4 \times 35$ mm were used in thermal shock tests. The material properties of alumina ceramics were measured and given in Table I. The thermal shock test system was customized, which was controlled by a computer to move the specimen between the hot zone of the furnace and the cooling bath. Heating and cooling temperature deviation of the thermal shock test system was within ± 3 °C. The alumina specimen was heated to the desired temperature for 15 min in the furnace and was quenched into the cooling liquid for 30 s in the bath. After quenching, the specimens were dried and the retained strength was measured by a universal testing machine (H10K-C, Hounsfield Test Equipment, UK) using a three-point bend fixture with a span of 30 mm and a crosshead speed of 0.5 mm/min.

TABLE I Properties of Al_2O_3 specimens

Density (g/cm^3)	3.8953
Mean strength (MPa)[a]	448.54
Mean grain size (μm)[b]	2.35
Fracture toughness (MPa·m$^{-1/2}$)[c]	4.8439

[a]Three-point bending strength.
[b]Mean grain size.
[c]SENB method.

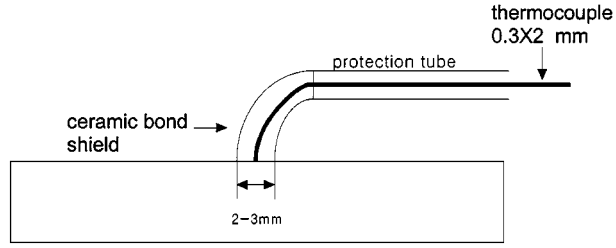

Figure 2 Schematic view of the thermocouple contact on the surface of the specimen for cooling rate measurement.

2.3. Measurement of the cooling rate

The temperature change of the specimen surface during quenching was measured by a K-type thermocouple of 0.3 mm diameter. The thermocouple was attached to the specimen surface and was fixed with a strong inorganic adhesive (Aron Ceramic D-5, Toagosei, Japan). The inorganic adhesive was optimally used to minimize the possible error during measurement. The figure of the temperature measurement is illustrated in Fig. 2. The thermocouple, which was attached to the specimen, was connected to a computer system equipped with a data acquisition system using an A/D converter (DT2835, Data Translation, USA) and the transient temperature was recorded into the computer storage. The sampling rate of data recording was 2000 Hz and the measuring period was 10 s.

3. Results and discussion

3.1. The effect of cooling rate in water

The measured surface temperature of the specimen which was heated to 220 °C in the furnace and quenched into distilled water of 20 °C (thermal shock temperature difference ΔT was 200 °C) is illustrated in Fig. 3a. To eliminate the signal noise, digital filter processing was carried out. After digital filtering, clear temperature change data could be obtained. Fig. 3b represents the temperature change plot against time after data filtering. The surface temperature of the specimen rapidly decreased immediately after immersed into the cooling water. However, the surface temperature of the specimen was decreased smoothly after 2 s.

Fig. 4 shows the surface temperature variations of the specimens which were heated to various high temperatures and quenched into the temperature of the cooling water 20 °C. The profiles of all surface temperature variations were analogous to each other. Therefore, it is very difficult to identify the characteristic difference of the cooling behaviour of the specimens from the profiles of temperature variations.

The cooling rates of the specimen surface for each quenching condition could be obtained by differentiation of the temperature variations with time. Fig. 5 shows both the surface temperature and cooling rate of the specimen surface during quenching into the water of temperature 20 °C against the cooling time when the

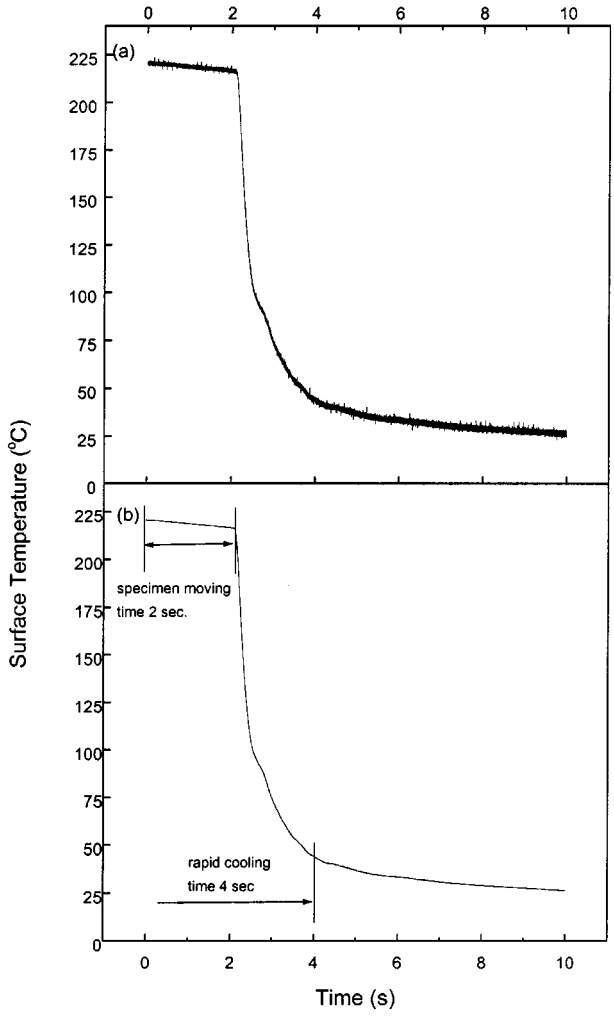

Figure 3 Temperature variation of the specimen surface as a function of time, when ΔT was 200 °C and the water temperature was 20 °C; (a) before filtering (b) after filtering.

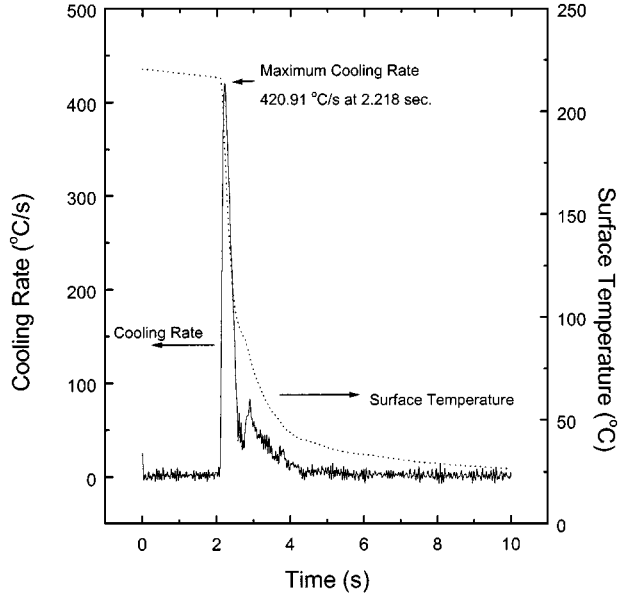

Figure 5 Cooling rate and surface temperature variation as a function of time, when ΔT was 200 °C and water temperature was 20 °C.

temperature difference ΔT was 200 °C. The cooling rate increased rapidly and reached the maximum cooling rate in 2.218 s for the cooling water of 20 °C as can be seen in Fig. 5. The maximum cooling rate was measured as 420.91 °C/s for $\Delta T = 200$ °C. The cooling rate of the specimen surface decreased after the maximum point because the heat transfer decreased as the surface temperature of the specimen decreased.

The maximum cooling rates for all temperatures of the cooling water and all thermal shock temperature differences are given in Fig. 6. For each temperature of the cooling water, the maximum cooling rate increased as the thermal shock temperature difference increased. In Fig. 7, the maximum cooling rates are represented

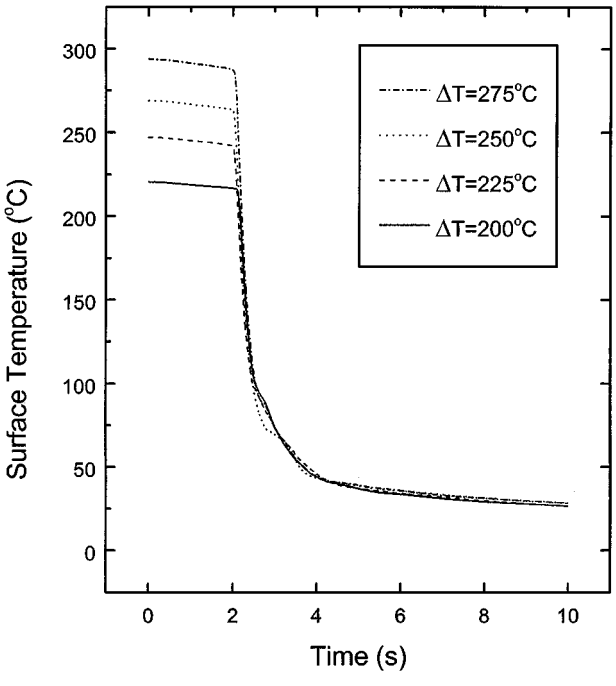

Figure 4 Temperature variation of the specimen surface as a function of time for various temperature differences, when water temperature was 20 °C.

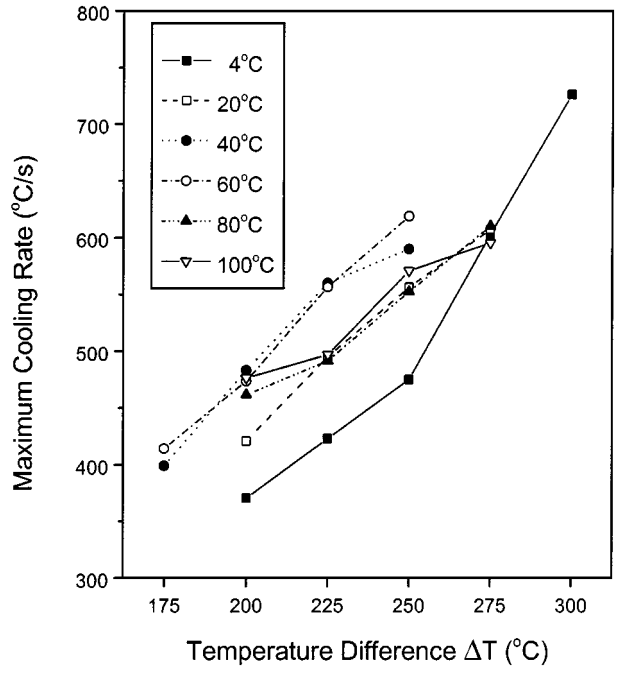

Figure 6 Maximum cooling rate as a function of temperature difference for various water temepratures.

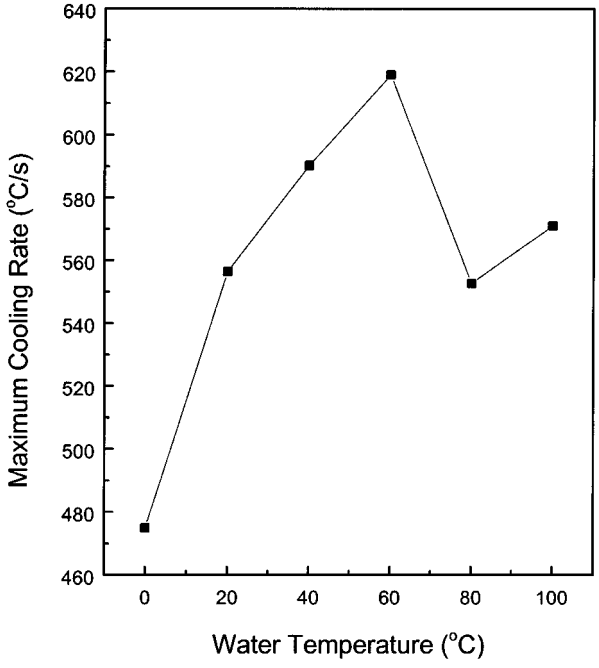

Figure 7 Maximum cooling rate as a function of water temperature at the fixed thermal shock temperature difference 250 °C.

as a function of the temperature of the cooling water for the same thermal shock temperature difference of 250 °C. From Fig. 7, it can clearly be understood that the maximum cooling rate increases as the temperature of the cooling water increases over the temperature range 4–60 °C, however, it decreases again over the temperature range 60–100 °C.

According to the lumped system analysis [12] the cooling rate of the specimen is proportional to the convection heat transfer coefficient as given in Equation 1,

$$q = hA[T_f - T(t)] = \rho C_p V \frac{dT(t)}{dt} \quad (1)$$

where, q is the heat transfer rate, h the convection heat transfer rate, A the surface area of the solid body, T_f the uniform temperature of the fluid, $T(t)$ the temperature of the surface of the solid body after time t s, ρ the density of the solid, C_p the specific heat of the solid body and V the volume of the solid.

Therefore, it can be said that the maximum cooling rate shown in Fig. 7 is proportional to the convection heat transfer coefficient. The fact that the maximum cooling rate increased over 4–60 °C and decreased again over 60–100 °C of the cooling water as shown in Fig. 7 can be explained by the characteristic behaviour of the convection heat transfer coefficient of water, as shown in Fig. 1. Up to 60 °C, it is considered that the specimen was cooled by natural-convection as illustrated in region I of Fig. 1 due to the fact that the heat transferred to the water from the specimen was not enough to boil the water. Hence, the convection heat transfer coefficient increased linearly with increasing temperature of water in this region. However, when the temperature of water increased above 60 °C, the water surrounding the specimen formed bubbles of vapour and the heat transfer mechanism changed to the nucleated boiling in region II and finally the heat transfer decreased remarkably by the film boiling as shown in region III of Fig. 1. Therefore, the convection heat transfer coefficients h_4, h_{20}, h_{40} and h_{60} for the temperatures of the cooling water 4, 20, 40 and 60 °C, respectively, can be expressed as Equation 2.

$$h_4 < h_{20} < h_{40} < h_{60} \quad (2)$$

Thermal stress of the plate specimen which is cooled at a constant cooling rate can be calculated by Equation 3 [13],

$$\sigma = \frac{Ea}{(1-\nu)} \cdot \frac{\phi \gamma_m^2}{3\alpha} \quad \text{(surface of the specimen)} \quad (3)$$

where, γ_m is the geometrical factor, α the thermal diffusivity and ϕ the cooling rate of the specimen. Equation 3 can not be applied to the whole range of thermal shock temperature difference because Equation 3 represents the thermal stress resulting from a constant cooling rate. However, the cooling rate is assumed to be constant for the differential element of time dt during which the differentiation of the temperature change with time d$T(t)$/dt is applied to Equation 1. Hence, a relationship between the thermal stress and the cooling rate can be expressed as Equation 4.

$$\sigma \propto \frac{dT}{dt} \quad (4)$$

Lumped system analysis gives Equation 5 from Equations 1 and 4.

$$\sigma \propto h \quad (5)$$

It can be, therefore, understood that both the thermal stresses σ_4, σ_{20}, σ_{40} and σ_{60}, and the maximum cooling rates ϕ_4, ϕ_{20}, ϕ_{40} and ϕ_{60} for the temperatures of cooling water 4, 20, 40 and 60 °C, respectively, can be expressed as Equations 6 and 7, respectively, for the same critical temperature difference because the thermal stress is proportional to the convection heat transfer coefficient, which is also proportional to the cooling rate of the specimen, as represented in Equation 3.

$$\sigma_4 < \sigma_{20} < \sigma_{40} < \sigma_{60} \quad (6)$$

$$\phi_4 < \phi_{20} < \phi_{40} < \phi_{60} \quad (7)$$

3.2. Effect of cooling rate in propylene glycol/water solutions

The quenching media of propylene glycol/water system were prepared by mixing propylene glycol by 25, 50 and 75 vol % into water. The surface temperature changes of the specimens during cooling in the bath of 25 vol % propylene glycol/water solution are plotted in Fig. 8 as a function of time for various thermal shock temperature differences between the temperature of the heated specimen surface and 20 °C of the cooling solution. The cooling tendency of the heated specimen

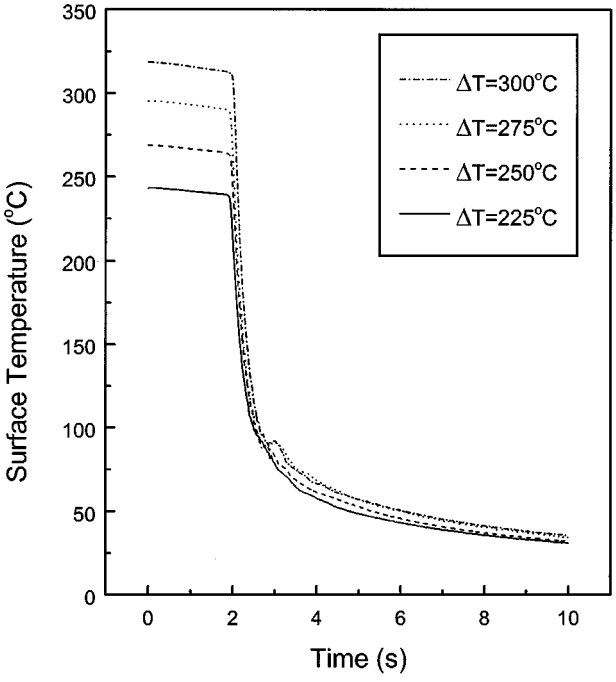

Figure 8 Temperature variation of the specimen surface as a function of time for various temperature differences, when 25 vol % propylene glycol aqueous solution was used as a cooling liquid.

surface in the propylene glycol/water solution, shown in Fig. 8, is analogous to that in the water, shown in Fig. 4.

The cooling rate of the specimen surface for each quenching condition of the propylene glycol/water solution was obtained by differentiation of the temperature variation curves of all specimens with time likewise for the cooling water. Hence, the maximum cooling rates during quenching into the propylene glycol/water solution of the temperature 20 °C are represented in Fig. 9 as a function of thermal shock temperature difference. The maximum cooling rate for zero vol % propylene glycol/water solution corresponds to that for the pure water of the same temperature 20 °C, as shown in Fig. 9.

Assuming that the convection heat transfer coefficient between the specimen and the cooling liquid is proportional to the cooling rate of the specimen surface as given in Equation 1, the convection heat transfer coefficients h_{p0}, h_{p25}, h_{p50} and h_{p75} for 0, 25, 50 and 75 vol % propylene glycol/water solutions, respectively, are considered to have a relationship as Equation 8.

$$h_{p0} > h_{p25} > h_{p50} > h_{p75} \tag{8}$$

In similar to Equations 6 and 7 for the cooling water, the thermal stresses σ_{p0}, σ_{p25}, σ_{p50} and σ_{p75}, and the maximum cooling rates ϕ_{p0}, ϕ_{p25}, ϕ_{p50} and ϕ_{p75} for 0, 25, 50 and 75 vol % of propylene glycol/water solutions, respectively, can be expressed as Equations 9 and 10, respectively, for the same thermal shock temperature difference because the thermal stress is proportional to the convection heat transfer coefficient, which is also proportional to the cooling rate of the specimen.

$$\sigma_{p0} > \sigma_{p25} > \sigma_{p50} > \sigma_{p75} \tag{9}$$

$$\phi_{p0} > \phi_{p25} > \phi_{p50} > \phi_{p75} \tag{10}$$

3.3. The effect of cooling rate on the critical thermal stress

When the three-point bending strength of the alumina specimens was measured after subjected to the thermal shock test by quenching into the cooling water, it was found that the critical temperature differences ΔT_C's were 275, 250, 225, 225, 250 and 250 °C for 4, 20, 40, 60, 80 and 100 °C of the cooling water, respectively, as shown in Fig. 10.

The critical temperature difference ΔT_C decreased as the temperature of the cooling water increased from

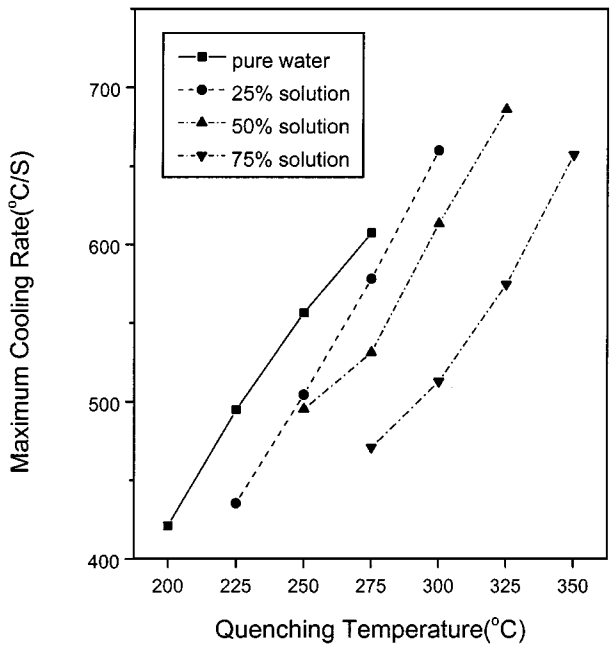

Figure 9 Maximum cooling rate as a function of temperature difference for various concentrations of propylene glycol aqueous solution.

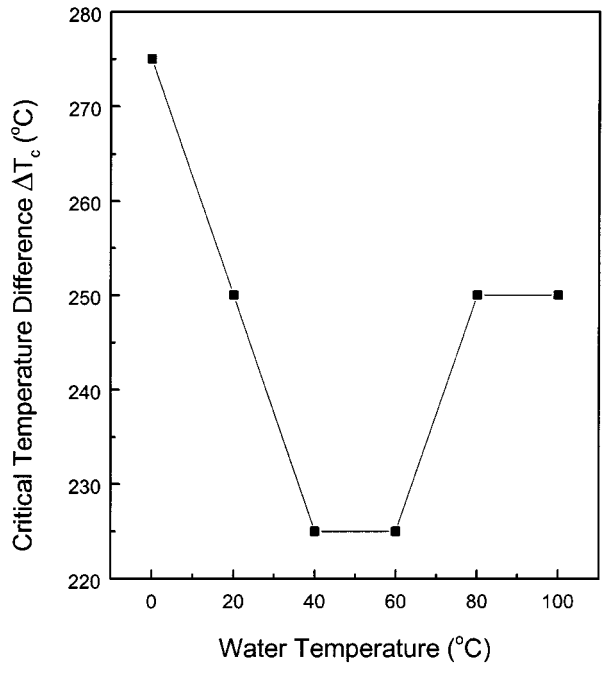

Figure 10 Critical temperature difference as a function of water temperature.

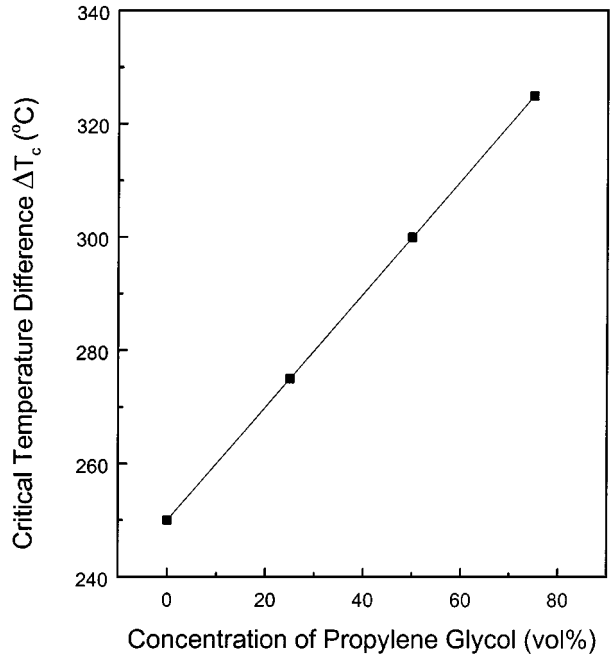

Figure 11 Critical temperature difference as a function of the concentration of propylene glycol aqueous solution.

4 °C up to 60 °C and increased again above 60 °C as shown in Fig. 10. This phenomenon is in good agreement with the tendency observed for the maximum cooling rate as shown in Fig. 7. When Fig. 7 is compared with Fig. 10 it can be understood that the higher the maximum cooling rate is, the lower the critical temperature difference is. If a specimen is subjected to the higher maximum cooling rate, it will suffer the thermal stress more severely and will need the less critical temperature difference for failure. This means that the maximum cooling rate determines the critical temperature difference of thermal shock.

The increase of the critical temperature difference above 60 °C as shown in Fig. 10 for water quenching is due to the decrease of the maximum cooling rate of the specimen above 60 °C, as can be seen in Fig. 7, because the maximum cooling rate is limited and decreases by the remarkable film boiling on the surface of the specimen at temperatures above 60 °C as discussed in Section 3.1.

The critical temperature difference for the propylene glycol/water solution increased linearly from 250 to 325 °C over the concentration range 0–75 vol % of propylene glycol/water solution of 20 °C, as shown in Fig. 11. The fact that the critical temperature difference for propylene glycol/water solution increased as the concentration of propylene glycol in water increased is due to the fact that the heat transfer coefficient of the solution as well as the cooling rate linearly decreases with increasing the concentration of propylene glycol in water.

3.4. The critical temperature difference and the critical cooling rate

A ceramic body is susceptible to catastrophic failure because of its general brittleness when it is subjected to a stress higher than the critical thermal stress [14]. The strength of a ceramic body degrades abruptly and fractures by crack growth caused by the critical thermal stress during thermal shock process likewise the mechanical stress by the mechanical loading. Both the temperature difference and the cooling rate generally cause the thermal stress [15]. Therefore, the temperature difference and the maximum cooling rate which generate the critical thermal stress and, hence, bring about the abrupt strength degradation are the critical temperature difference and the critical (maximum) cooling rate, respectively.

The maximum cooling rates for the various temperatures of the cooling water are represented in Fig. 12 as a function of the quenching temperature difference. The critical thermal shock temperature differences are represented as circled data points for the respective temperature differences in Fig. 12. It can be understood from Fig. 12 that all critical thermal shock temperature differences are above and very close to a certain value of the cooling rate 550 °C/s. The maximum cooling rates for the respective concentrations of propylene glycol in water are represented in Fig. 13 as a function of the quenching temperature difference. The critical thermal shock temperature differences are represented as circled data points for the respective temperature differences in Fig. 13. It can also be understood from Fig. 13 that all critical thermal shock temperature differences are above and very close to the same value of the cooling rate 550 °C/s as that for the cooling water. The critical cooling rates of the specimen surface are considered to be above the value 550 °C/s for all different thermal shock conditions. This means that the cooling rates of all specimens that make the cracks grow catastrophically should be higher than the critical cooling rate, 550 °C/s, for all thermal shock tests in this study of alumina ceramics.

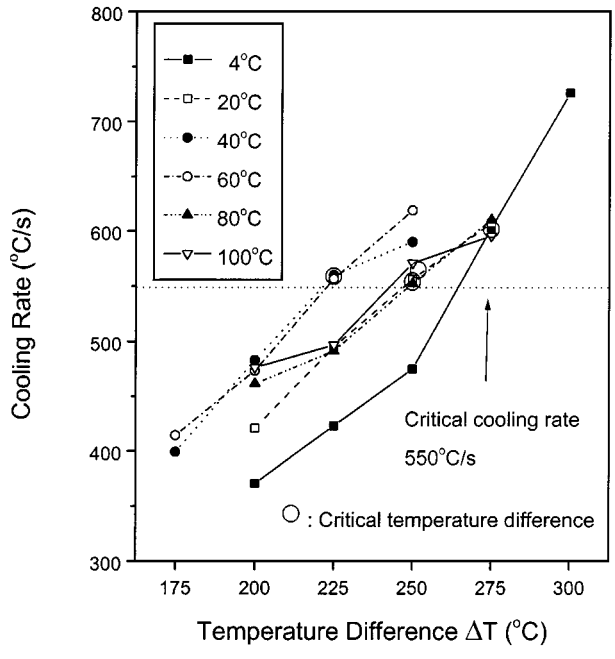

Figure 12 Maximum cooling rate as a function of temperature difference for various water temperatures.

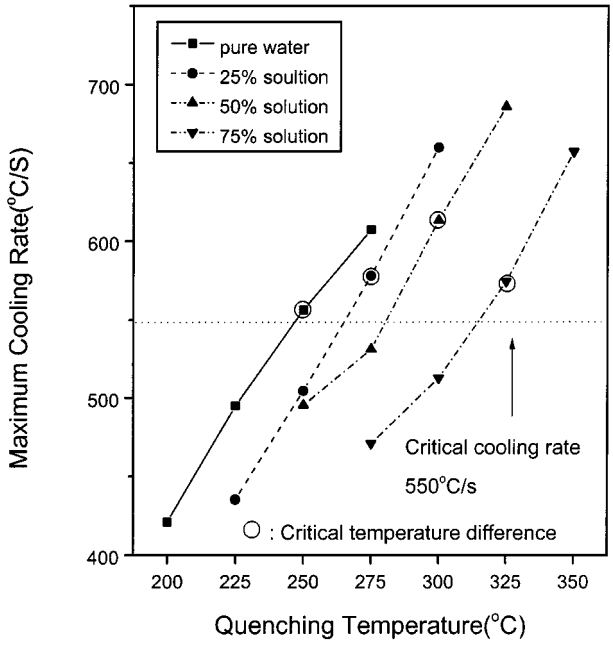

Figure 13 Maximum cooling rate as a function of temperature difference for various concentrations of propylene glycol aqueous solution.

The strength degradation of a solid specimen is only dependent upon the thermal stress if there is no other thermal deformation except thermal expansion and contraction during the thermal shock process. Since the thermal stress works just like the mechanical stress, the thermal stress which makes the cracks grow by critical thermal shock temperature difference should be the same with the stress σ_C of Equation 11 [16].

$$K_{IC} = Y\sigma_C\sqrt{C} \tag{11}$$

where, K_{IC} is the critical stress intensity factor, Y the shape factor of the crack, C the crack length, σ_C the critical thermal stress which makes the cracks grow catastrophically. The critical thermal stress which makes the cracks grow catastrophically is generated by the critical cooling rate. The cooling rate which generates the critical thermal stress is defined as the critical cooling rate. The critical cooling rate of alumina ceramics is considered to be 550 °C/s in this study.

From the results obtained in this study, it can be said that the critical thermal shock temperature difference is dependent on the cooling rate. However, the cooling rates for all critical thermal shock temperature differences in this study approached the critical cooling rate, which is considered to be most influential of the environmental factors on the thermal shock behaviour of the ceramic bodies.

4. Conclusions

The maximum cooling rate of the alumina ceramics was obtained by measuring the surface temperature of the alumina specimens during quenching into the various temperatures of water and the propylene glycol/water solutions. The effect of the cooling rate on the thermal shock behaviour of alumina ceramics was studied and the results are summarized as follows:

(1) The maximum cooling rate increased as the thermal shock temperature difference increased for each temperature of the cooling water. For the same thermal shock temperature difference, the maximum cooling rate increased as the temperature of the cooling water increased over the temperature range 4–60 °C, but the reverse for the higher temperature range 60–100 °C due to the remarkable film boiling.

The convection heat transfer coefficients h_4, h_{20}, h_{40} and h_{60} for the temperatures of the cooling water 4, 20, 40 and 60 °C, respectively, can be expressed as: $h_4 < h_{20} < h_{40} < h_{60}$. The thermal stresses σ_4, σ_{20}, σ_{40} and σ_{60}, and the maximum cooling rates ϕ_4, ϕ_{20}, ϕ_{40} and ϕ_{60} for the temperatures of cooling water 4, 20, 40 and 60 °C, respectively, can be expressed; $\sigma_4 < \sigma_{20} < \sigma_{40} < \sigma_{60}$ and $\phi_4 < \phi_{20} < \phi_{40} < \phi_{60}$, for the same thermal shock temperature difference because the thermal stress is proportional to the convection heat transfer coefficient, which is also proportional to the cooling rate of the specimen.

(2) The convection heat transfer coefficients h_{p0}, h_{p25}, h_{p50} and h_{p75} for 0, 25, 50 and 75 vol % propylene glycol/water solutions, respectively, were found to have the relationship: $h_{p0} > h_{p25} > h_{p50} > h_{p75}$. The thermal stresses σ_{p0}, σ_{p25}, σ_{p50} and σ_{p75}, and the maximum cooling rates ϕ_{p0}, ϕ_{p25}, ϕ_{p50} and ϕ_{p75} for 0, 25, 50 and 75 vol % of propylene glycol/water solutions, respectively, can be expressed as: $\sigma_{p0} > \sigma_{p25} > \sigma_{p50} > \sigma_{p75}$ and $\phi_{p0} > \phi_{p25} > \phi_{p50} > \phi_{75}$, for the same thermal shock temperature difference as the same reason with the pure cooling water.

The critical temperature difference increased almost linearly as the concentration of the propylene glycol in water increased, probably because the heat transfer coefficient linearly decreases with increasing the concentration of propylene glycol in water.

(3) The critical thermal stress which makes the cracks grow catastrophically is generated by the critical cooling rate. The critical cooling rate of alumina ceramics was found to be 550 °C/s in this study.

From the results obtained in this study, it can be said that the critical thermal shock temperature difference is dependent on the cooling rate. However, the cooling rates for all critical thermal shock temperature differences approached the critical cooling rate, which is considered to be most influential of the environmental factors in the thermal shock behaviour of the alumina ceramics.

Acknowledgement

This work was supported by Yonsei University Research Fund of 1997.

References

1. D. P. H. HASSELMAN, *J. Amer. Ceram. Soc.* **53** (1970) 490.
2. H. WANG and R. N. SINGH, *Int. Mater. Review* **39** (1994) 228.
3. S. S. MANSON, "Thermal Stress and Low-Cycle Fatigue" (McGraw-Hill, New York, 1966) p. 275.
4. M. NECATI ÖZISIK, "Heat Transfer A Basic Approach" (McGraw-Hill, New York, 1985) p. 5.

5. T. HISIKAWA, T. GAO, M. HIBI, M. TAKATSU and M. OGAWA, *J. Mater. Sci.* **29** (1994) 213.
6. Y. KIM, W. J. LEE and E. D. CASE, *Mater. Sci. Eng.* **A145** (1991) L7.
7. J. P. SINGH, J. R. THOMAS and D. P. H. HASSELMAN, *J. Amer. Ceram. Soc.* **63** (1980) 140.
8. P. F. BECHER, *Comm. Amer. Ceram. Soc.* **64** (1981) C-17.
9. P. F. BECHER, D. LEWIS III, K. R. CARMAN and A. C. GONZALEZ, *Amer. Ceram. Soc. Bull.* **59** (1980) 542.
10. M. NECATI ÖZISIK, "Heat Transfer A Basic Approach" (McGraw-Hill, New York, 1985) p. 492.
11. CRC Handbook of Chemistry and Physics, edited by D. R. Lide, 75th ed. (CRC Press, London, 1994) pp. 6–249.
12. M. NECATI ÖZISIK, "Heat Transfer: A Basic Approach" (McGraw-Hill, New York, 1985) p. 102.
13. W. D. KINGERY, *J. Amer. Ceram. Soc.* **38** (1995) 3.
14. H. W. HAYDEN, W. G. MOFFATT and J. WULFF, in "The Structure and Properties of Materials" (John Wiley & Sons, New York, 1965) p. 143.
15. D. P. H. HASSELMAN, *Ceram. Bull.* **49** (1970) 1033.
16. R. W. DAVIDGE, "Mechanical Behavior of Ceramics" (Cambridge University Press, London, 1979) p. 38.

Received 31 August 1998
and accepted 29 January 1999